Time-Frequency Compressed Spectrum Sensing in Cognitive Radios

Shaghayegh S.M. Monfared*, Abbas Taherpour* and Tamer Khattab**
*Department of Electrical Engineering, Imam Khomeini International University, Qazvin, Iran
**College of Engineering, Qatar University, Doha, Qatar
{shaghayegh_shakoori, taherpour}@ikiu.ac.ir and tkhattab@qu.edu.qa

***Abstract*—In this paper, we investigate the use of time-frequency analysis for improvement of spectrum sensing in cognitive radios and exploit compressed sensing (sampling) to reduce the extremely high sampling rate of signal in time-frequency plane. We suggest a non-parametric spectrum sensing technique similar to energy detection utilizing time-frequency analysis to generally compromise between accuracy and sensing time, though the computational cost is significantly increased. As the representation of signals on the time-frequency plane is intrinsically sparse, thus we use the compressed sensing to achieve a significant reduction in the number of measurements. We propose using of different time-frequency representation such as short time Fourier transform, wavelet, Wigner-Ville and pseudo Wigner-Ville distribution in conduction of compressed sampling technique. The simulation results evaluate the performance of the proposed time-frequency compressed detectors compared to other time-frequency and energy detectors using basis pursuit and Bayesian compressive sensing reconstruction algorithms for AWGN and also Rayleigh and Rician fading channels.**

I. Introduction

In cognitive radios (CRs), spectrum sensing detects the presence or absence of a primary user (PU) on an associated spectrum. The secondary users (SUs) should perform the fast and accurate spectrum sensing to increase the spectral efficiency and also avoid causing interference to PU, Thus spectrum sensing plays a fundamental and significant role in cognitive radio networks. Traditionally, the spectrum sensing techniques look for possible spectrum holes in frequency domain. However, the time dimension is also important for the cognitive radio receiver to sense the type of modulation employed by the PU. Therefore, we can achieve more accurate spectrum sensing by using both domains simultaneously which is considered as the time-frequency (TF) analysis. A time-frequency representation (TFR) obtains the energy density of a signal simultaneously in the time and frequency and therefore. provides an accurate picture of energy distribution and in addition an ideal tool to analyze the non-stationary signals. As the notable TFRs, we may mention the short time Fourier transform (STFT), the wavelet transform and the Wigner-Ville distribution (WVD) [1], [2]. In the context of spectrum sensing in CRs recently, there have been several related works to develop the efficient spectrum sensing techniques by using TFRs [3]–[6]. In [4], a spectrum sensing technique is considered based on a joint TF detection of PU signal that the proposed technique is more reliable than classical energy detection in time or frequency plane. In [5], a novel non-parametric spectrum sensing approach exploiting the TF analysis has been suggested which leads to the improvements in temporal and spectral resolution. In [6], a new energy detector is proposed which the spectrum sensing algorithm is implemented by using discrete wavelet transform and the proposed detector performs faster than the conventional energy detectors.

However in practice, we face a major implementation challenge in TF spectrum sensing that lies in the great number of samples in the TF plane. The power localization property in joint-domain representations renders the signals sparse in the TF (Wigner-Ville, wavelets, etc.) and ambiguity domains. For most of the signals in real applications, the TF representation contains a small number of non-zero values, so we can use the compressed sensing (CS) to achieve fast spectrum sensing and significant reduction in the number of measurements [7]–[9]. Recently, TF localization has been considered based on CS [10], [11]. Furthermore, the robust CS algorithm is applied to the ambiguity domain to achieve the high resolution TF representation in impulse noise [12], [13]. Also, [14] introduces a useful technique for the measurement process of the TF shifts system based on CS and [15] investigates recovery conditions for sparse time-frequency representations. In the context of compressed spectrum sensing, the existing studies focus only on a single domain representation, thus we propose a new method for developing the compressed spectrum sensing by utilizing TFRs.

In this paper, we assume that the PU signal has sparse representation in the TF domain and then propose a non-parametric spectrum sensing technique based on TF analysis, which also utilizes the CS. A non-parametric spectrum sensing technique such as energy detection is suggested to generally make a trade off between accuracy and the sensing time. Although, using TF analysis in spectrum sensing increases the computational cost, we can use the CS to achieve a significant reduction in the number of measurements. The simulation results evaluate the performance of the proposed TF compressed detectors compared to energy detectors based on fast Fourier transform (FFT) and various TF representations [5]. In all simulations, we use the digital TV (DTV) PU signal as in IEEE 802.22 wireless regional area network (WRAN) systems. Furthermore, the performance of our detectors is presented with CS reconstruction algorithms such as basis pursuit (BP) [16] and Bayesian compressive sensing (BCS)

978-1-4799-1353-4/13/$31.00 ©2013 IEEE

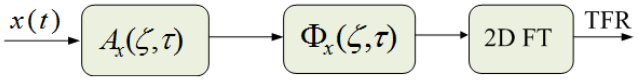

Fig. 1: Block diagram of quadratic TFRs.

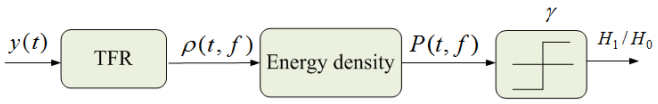

Fig. 2: System model of the TF non-parametric spectrum sensing.

[17] under additive white Gaussian noise (AWGN) and also Rayleigh and Rician fading channels.

The rest of the paper is organized as follows. Section II presents the theoretical background of CS and quadratic TF analysis. In Section III, we investigate the use of TF analysis in non-parametric spectrum sensing and then we propose a new TF non-parametric spectrum sensing by exploiting CS. Finally, simulation results and conclusions are considered in Sections IV and V, respectively.

Notation: We use lightface letters for scalars, and boldface uppercase and lowercase letters for matrices and vectors respectively.

II. Theoretical Background

A. Compressed Sensing

Let $x(t)$ be the analog signal that a digital receiver converts it to a discrete-time signal $\mathbf{x} = [x_1, x_2, ..., x_N]^T \in \mathbb{C}^{N\times 1}$ (here $(.)^T$ denotes the transpose operation). According to CS theories, $\mathbf{x}$ is S-sparse in basis matrix $\mathbf{\Psi}$, if $\mathbf{x} = \mathbf{\Psi a}$, where $\mathbf{\Psi}$ is a $N \times N$ matrix and $\mathbf{a}$ is a $N \times 1$ vector with only $S \ll N$ non-zero elements. In CS, a random measurement matrix $\mathbf{\Phi} \in \mathbb{C}^{P\times N}$ is used to sample the signal instead of Nyquist sampling, where $P \leq N$. Then the measurement vector $\mathbf{y} = [y_1, y_2, ..., y_P]^T \in \mathbb{C}^{P\times 1}$ is obtained by $\mathbf{y} = \mathbf{\Phi x} = \mathbf{\Phi\Psi a}$. The restricted isometry property (RIP) of a measurement matrix $\mathbf{\Phi}$ provides adequate performance of the sensing system and plays important role in CS. The matrix $\mathbf{\Phi}$ obeys the RIP of order S if there exists an isometry constant $\delta_S \in (0, 1)$, such that

$$(1 - \delta_S) \|\mathbf{x}\|_2^2 \leq \|\mathbf{\Phi x}\|_2^2 \leq (1 + \delta_S) \|\mathbf{x}\|_2^2 \qquad (1)$$

holds for all S-sparse vectors. $\|\mathbf{x}\|_2$ is the ℓ_2-norm of the vector $\mathbf{x}$ that is equal to the $(\sum_{i=1}^{N} |x_i|^2)^{1/2}$. The simplest example of a measurement matrix $\mathbf{\Phi}$ whose entries $\phi_{i,j}$ are drawn independently from a Gaussian source [7].

Finally, the sparse vector $\mathbf{a}$ can be recovered from the measurement vector $\mathbf{y}$ with high probability by solving the ℓ_1-norm optimization problem as follows:

$$\hat{\mathbf{a}} = \arg\min_{\mathbf{a}} \|\mathbf{a}\|_1 \quad \text{s.t.} \quad \mathbf{y} = \mathbf{\Phi\Psi a}. \qquad (2)$$

If $P \geq c.S\log(N/S)$, where c is constant. Therefore, we can use the linear programming techniques, e.g., ℓ_1-minimization (Basis Pursuit) [16], or iterative greedy algorithms [18] to solve this equation.

B. Quadratic Time-Frequency Analysis

In this paper, we concentrate on the spectrogram (SP), scalogram (SC), WVD that are considered as the quadratic time-frequency representations. The SP can be defined as the squared modulus of the STFT. Also, the SC is the squared modulus of the continuous wavelet transform (CWT) that is an energy distribution of the signal in the time-scale plane. In general, the TF energy distributions belong to the quadratic representations. The quadratic TFRs, known as Cohen's class can be formulated as [1]

$$\rho_x(t, f) = \int\int A_x(\xi, \tau)\Phi_x(\xi, \tau)e^{j2\pi(\xi t - f\tau)}\mathrm{d}\tau\mathrm{d}\xi, \qquad (3)$$

where $A_x(\xi, \tau)$ and $\Phi_x(\xi, \tau)$ are called the ambiguity function (AF) and the kernel of the distribution, respectively. The AF measures the TF correlation of a signal. Due to the fact that the ambiguity domain is a two-dimensional (2D) Fourier transform of the WVD, we can express any quadratic TFR as a function of the WVD. Therefore, the AF plays a key role in the TF analysis, and is given by

$$A_x(\xi, \tau) = \int x(u + \frac{\tau}{2})x^*(u - \frac{\tau}{2})e^{-j2\pi\xi u}\mathrm{d}u, \qquad (4)$$

where $x(t)$ represents the analysed signal. ξ and τ are relative coordinates that are called Doppler frequency and time delay, respectively. By taking the 2D Fourier transform of the multiplication of $A_x(\xi, \tau)$ and $\Phi_x(\xi, \tau)$, a quadratic TFR can be also obtained as

$$\rho_x(t, f) = \underset{\tau\to f}{\mathcal{F}} \; \underset{\xi\to t}{\mathcal{F}^{-1}} \left[A_x(\xi, \tau).\Phi_x(\xi, \tau)\right]. \qquad (5)$$

This operation is equivalent to a 2D filtering in the ambiguity domain. Its block diagram is illustrated in Figure 1. By choosing a particular kernel function, we can generate a new quadratic TFR. For instance, the WVD is defined by selecting the kernel as unit, $\Phi_x(\xi, \tau) = 1$. Another example is the SP, so that its kernel is defined as the ambiguity function of an arbitrary window function, $\Phi_x(\xi, \tau) = A_h^*(\xi, \tau)$ [2]. Also, the SC kernel is $\Phi_x(\alpha, \beta) = WVD_\Psi(\alpha/f_0, f_0\beta)$, where $\Psi(f)$ is the Fourier transform of mother wavelet $\psi(t)$ and f_0 is a central frequency [19].

III. Time-Frequency Spectrum Sensing Based CS

In this section, we suggest a new TF non-parametric spectrum sensing by exploiting CS to extremely reduce the number of samples in the TF plane. But at first, we investigate the non-parametric spectrum sensing problem with different TFRs.

A. Non-Parametric Spectrum Sensing With TF Analysis

We use the TF analysis tools for carrying out the non-parametric spectrum sensing such as energy detection and illustrate the system model in Figure 2. This non-parametric spectrum sensing technique is considered for its significant

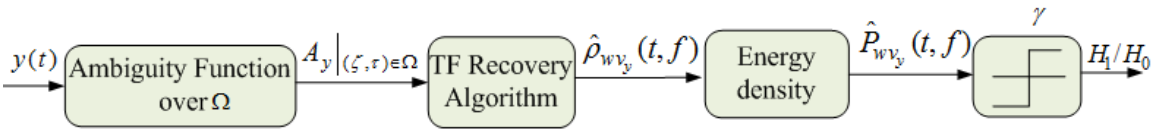

Fig. 3: Compressed spectrum sensing model based on WVD.

performance and compromises between accuracy and the sensing time to detect the PU signal. The received signal $y(t)$ contains the PU signal $x(t)$ that corrupted by noise $n(t)$ as

$$y(t) = x(t) + n(t). \tag{6}$$

At first, we calculate the energy density of the received signal using TF analysis for the two cases. The S_0, where only noise is being received and the S_1 for case where the received signal includes the PU signal and noise. The S_0 and S_1 are the random variables, but the type of their distributions is not obvious and depends on the type of noise and the TF analysis used in the energy density. For instance, the energy density of the received signal using SC can be obtained as

$$P_{sp_y}(t,f) = \Big| \int y(\tau) h^*(t-\tau) e^{-j2\pi f\tau} \mathrm{d}\tau \Big|^2, \tag{7}$$

where $h(t)$ is a short time analysis window. The S_{sp_0} and S_{sp_1} are simply as

$$S_{sp_0} = \Big| \int n(\tau) h^*(t-\tau) e^{-j2\pi f\tau} \mathrm{d}\tau \Big|^2, \tag{8}$$

and

$$S_{sp_1} = S_{sp_0} + \Big| \int x(\tau) h^*(t-\tau) e^{-j2\pi f\tau} \mathrm{d}\tau \Big|^2. \tag{9}$$

Also, we can compute the energy density of the received signal using Scalogram as follows:

$$P_{sc_y}(a,b) = \Big| \frac{1}{\sqrt{|a|}} \int y(t) \Psi^*\big(\frac{t-b}{a}\big) \mathrm{d}t \Big|^2, \tag{10}$$

where constant $a(>0)$ is the dilation parameter and b is the shift parameter. Then, we can obtain S_{sc_0} and S_{sc_1} as

$$S_{sc_0} = \Big| \frac{1}{\sqrt{|a|}} \int n(t) \Psi^*\big(\frac{t-b}{a}\big) \mathrm{d}t \Big|^2, \tag{11}$$

and

$$S_{sc_1} = S_{sc_0} + \Big| \frac{1}{\sqrt{|a|}} \int x(t) \Psi^*\big(\frac{t-b}{a}\big) \mathrm{d}t \Big|^2. \tag{12}$$

The WVD is also considered for computing the energy density of the received signal as

$$P_{wv_y}(t,f) = \Big| \int y(t+\frac{\tau}{2}) y^*(t-\frac{\tau}{2}) e^{-j2\pi f\tau} \mathrm{d}\tau \Big|^2. \tag{13}$$

The S_{wv_0} and S_{wv_1} can be obtained as

$$S_{wv_0} = \Big| \int n(t+\frac{\tau}{2}) n^*(t-\frac{\tau}{2}) e^{-j2\pi f\tau} \mathrm{d}\tau \Big|^2, \tag{14}$$

and

$$S_{wv_1} = \Big| \int x(t+\frac{\tau}{2}) x^*(t-\frac{\tau}{2}) e^{-j2\pi f\tau} \mathrm{d}\tau \Big|^2 + S_{wv_0} + 2Re\{S_{wv_{01}}\}, \tag{15}$$

where $S_{wv_{01}}$ are the cross terms and are defined as

$$S_{wv_{01}} = \Big| \int n(t+\frac{\tau}{2}) x^*(t-\frac{\tau}{2}) e^{-j2\pi f\tau} \mathrm{d}\tau \Big|^2. \tag{16}$$

The cross-terms in the WVD can disturb the readability of the signal representation, hence we use the pseudo WVD (PWVD) to attenuate the interferences and compute the energy density of the received signal as [20]

$$P_{pw_y}(t,f) = \Big| \int h(\tau) y(t+\frac{\tau}{2}) y^*(t-\frac{\tau}{2}) e^{-j2\pi f\tau} d\tau \Big|^2. \tag{17}$$

The S_{pw_0} and S_{pw_1} can be defined as

$$S_{pw_0} = \Big| \int h(\tau) n(t+\frac{\tau}{2}) n^*(t-\frac{\tau}{2}) e^{-j2\pi f\tau} d\tau \Big|^2, \tag{18}$$

and

$$S_{pw_1} = \Big| \int h(\tau) x(t+\frac{\tau}{2}) x^*(t-\frac{\tau}{2}) e^{-j2\pi f\tau} d\tau \Big|^2 + S_{pw_0} + 2Re\{S_{pw_{01}}\}, \tag{19}$$

where the cross-terms are calculated as

$$S_{pw_{01}} = \Big| \int h(\tau) n(t+\frac{\tau}{2}) x^*(t-\frac{\tau}{2}) e^{-j2\pi f\tau} d\tau \Big|^2. \tag{20}$$

Finally, we apply the maximum likelihood test to detect the absence and presence of the PU signal in a particular frequency band at a specific time instant that are represented by $\mathcal{H}_0$ and $\mathcal{H}_1$, respectively. Thus, the detection problem can be expressed as the following binary hypothesis test [5]:

$$\begin{cases} \mathcal{H}_0: & P_y(t,f) < \eta, \\ \mathcal{H}_1: & P_y(t,f) > \eta, \end{cases} \tag{21}$$

where η is the sensing threshold. We select η to give minimum error in hypothesis testing, thus we equate the probability of false alarm P_{fa} and the probability of missed detection P_{m} in the ROC (receiver operating characteristics) curve.

Since the TF analysis simultaneously enhances the temporal and spectral resolution, TF spectrum sensing gives much improved results over other spectrum sensing approaches and requires smaller sensing time to detect the presence of a primary user. However, the computational complexity of this kind of TF spectrum sensing is very high rather than single domain ones so that it may not work well for wideband signals and we need to develop a new algorithm with lower computational complexity.

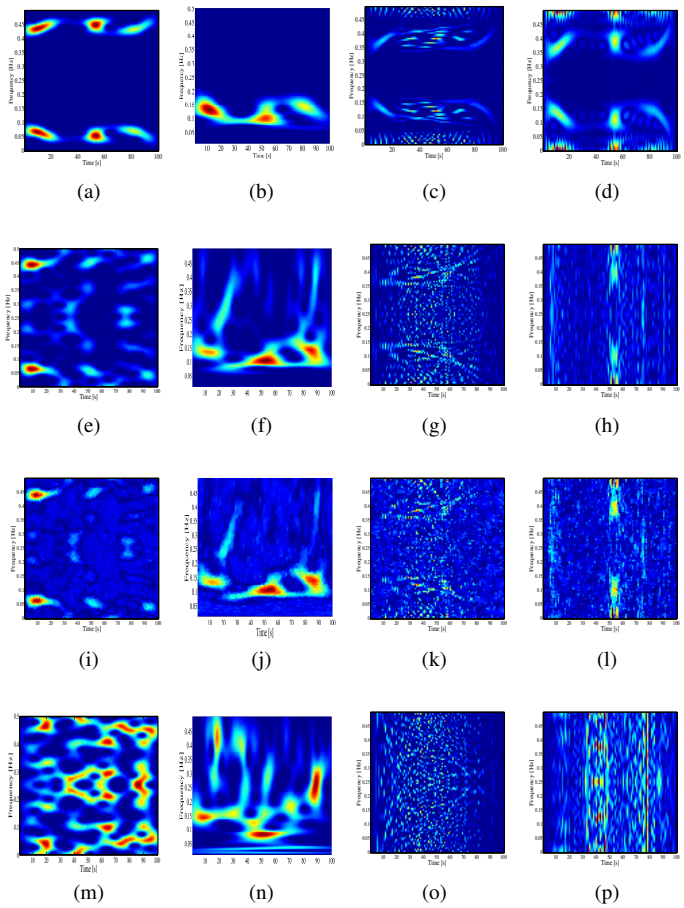

Fig. 4: The quadratic TFR of DTV signal in noise-free case (a) Spectrogram (b) Scalogram (c) WVD (d) PWVD, and the quadratic TFR of DTV signal for $\mathrm{SNR} = -5\,\mathrm{dB}$ (e) Spectrogram (f) Scalogram (g) WVD (h) PWVD, and the recovery of the quadratic TFR of DTV signal by minimizing the ℓ_1-norm for $\mathrm{card}(\Omega)/N^2 = 0.25$ (i) Spectrogram (j) Scalogram (k) WVD (l) PWVD, and the quadratic TFR of DTV signal for $\mathrm{SNR} = -20\,\mathrm{dB}$ (m) Spectrogram (n) Scalogram (o) WVD (p) PWVD.

B. Proposed Compressed Spectrum Sensing Algorithm

We propose a new non-parametric spectrum sensing algorithm based on the CS with considering sparsity constraint in TF plane. Let the analyzed signal be discrete-time with N sample, thus its TFR has N^2 samples over N frequency bins. The number of non-zero components K is much smaller than the signal samples ($K \ll N$), consequently $K.N$ components are expected to be non-zero in TF plane. Hence we can suppose that the TFR of signal is very sparse and utilize the CS based on TF analysis.

At first, we select a suitable collection of AF samples neighboring the origin of the plane in a given domain $\Omega(\xi, \tau)$. Then we must search for the sparsest TFR ρ such that its 2D Fourier transform $\mathcal{F}\{\rho\}$ coincides with the original AF over Ω [10], [11]. Hence a near-optimal sparse recovery can be considered to solve a linear program by minimizing the ℓ_1-norm. The TF distribution of the received signal can be obtained as

$$\begin{aligned} &\hat{\rho}_y = \arg\min_{\rho_y} \|\rho_y\|_1 \\ &\text{s.t.} \underset{\tau\to f}{\mathcal{F}} \underset{\xi\to t}{\mathcal{F}^{-1}} \left[A_y.\Phi_y\right] - \rho_y = 0|_{(\xi,\tau)\in\Omega}, \end{aligned} \tag{22}$$

where Φ_y is a kernel function. The domain Ω has different area and shape, but its cardinality should be [21]

$$\mathrm{card}(\Omega) \geq c.K.N.\log(N^2) \tag{23}$$

to recover exactly K of N points in a TF domain of size N^2 through ℓ_1 minimization. We assume that the area of a domain is a fixed square which is geometrically matched to the structure of the AF near the origin and makes the simplest solution.

Figure 3 illustrates the compressed spectrum sensing algorithm based on WVD. It is important to first determine the origin of the AF plane and choose a suitable domain. Implementation of this algorithm can be presented as four following steps:

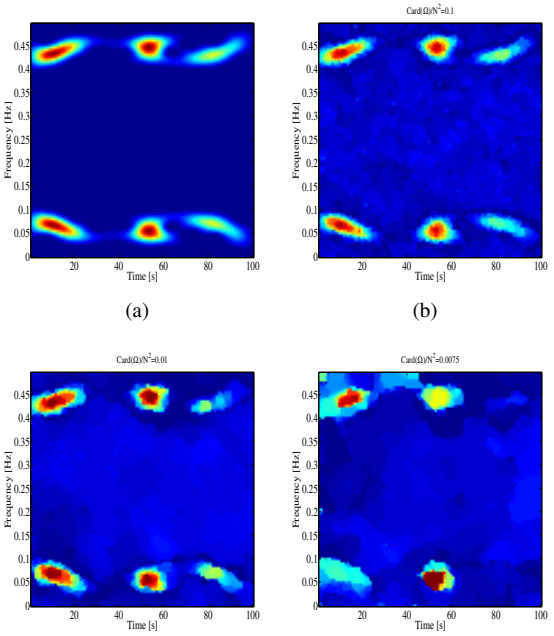

Fig. 5: (a) The SP of DTV signal in noise-free case; the recovery of the SP of DTV signal by minimizing the ℓ_1-norm for (b) $\mathrm{card}(\Omega)/N^2 = 0.1$, (c) $\mathrm{card}(\Omega)/N^2 = 0.01$, (d) $\mathrm{card}(\Omega)/N^2 = 0.0075$.

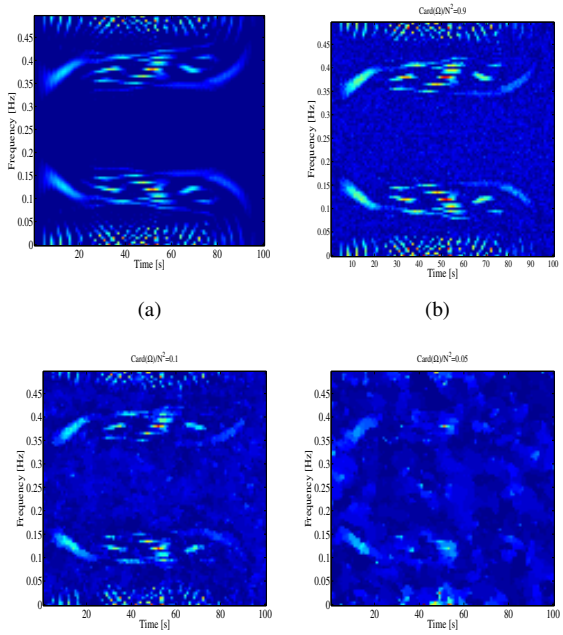

Fig. 6: (a) The WVD of DTV signal in noise-free case; the recovery of the WVD of DTV signal by minimizing the ℓ_1-norm for (b) $\mathrm{card}(\Omega)/N^2 = 0.9$, (c) $\mathrm{card}(\Omega)/N^2 = 0.25$, (d) $\mathrm{card}(\Omega)/N^2 = 0.05$.

1) Select suitable collection of AF samples neighboring the origin of the plane in a given domain Ω.
2) Estimation of Wigner-Ville distribution of the received signal by the ℓ_1-minimization problem as [11]

$$\begin{aligned} \hat{\rho}_{wv_y} &= \arg\min_{\rho_{wv_y}} \left\|\rho_{wv_y}\right\|_1 \\ \text{s.t.} \quad & \mathcal{F}\{\rho_{wv_y}\} - A_y = 0|_{(\xi,\tau)\in\Omega}. \end{aligned} \tag{24}$$

3) Compute the energy density of the received signal by using the WVD as follows:

$$\hat{P}_{wv_y}(t,f) = \left|\hat{\rho}_{wv_y}(t,f)\right|^2. \tag{25}$$

4) Detect the absence and presence of the PU signal in a frequency band by following binary hypothesis test:

$$\begin{cases} \mathcal{H}_0: & \hat{P}_{wv_y}(t,f) < \eta_{wv}, \\ \mathcal{H}_1: & \hat{P}_{wv_y}(t,f) > \eta_{wv}, \end{cases} \tag{26}$$

where η_{wv} is the sensing threshold.

Although the computational complexity and sensing time are decreased based on proposed algorithm, however the performance will be degraded with lower sample concentrations as well. In order to restore and improve the performance of proposed detectors, we can utilize the robust reconstruction algorithm such as BCS, instead of the BP.

IV. Simulation Results

In this section, all the provided simulation results have been made in MATLAB, with the TIME FREQUENCY TOOLBOX [22] for the TF computations and the ℓ_1-MAGIC TOOLBOX [23] for the optimization. The proposed detection method is discussed for a 100-point DTV signal, so the TF plane has 100×100 samples over 100 frequency bins. In all simulation, the spectrogram is produced from a 128-point short-time Fourier Transform. Also, the SC is defined as the squared magnitude of the 12-point Morlet wavelet. The simulations have been done assuming additive white Gaussian noise (AWGN) model.

In Figure 4, we compare the quadratic TFRs of DTV signal in noise-free, $\mathrm{SNR} = -5\,\mathrm{dB}$ and $\mathrm{SNR} = -20\,\mathrm{dB}$. In general, the SP is a cross-terms free TF distribution, however suffers from the undesirable trade-off between time and frequency concentration. As can be seen, the SC has a better time resolution compared to SP. Also, the WVD gives high resolution in time and frequency domain and is invariant to the window effects, but it includes drawbacks that so called cross-terms. In $\mathrm{SNR} = -5\,\mathrm{dB}$, the use of the WVD leads to the problem of cross-terms which can disturb the readability of the signal representation. Thus, we use the PWVD to attenuate the effects of cross-terms and has a high TF resolution at the same time. In addition, we illustrate the recovery of the different noisy quadratic TFRs by minimizing the ℓ_1-norm for $\mathrm{card}(\Omega)/N^2 = 0.25$. As can be observed, the recovery of the WVD of DTV signal includes more undesired cross-terms rather than other TFRs. At last, we plot the quadratic TFRs of DTV signal at $\mathrm{SNR} = -20\,\mathrm{dB}$. The energy of signal can not

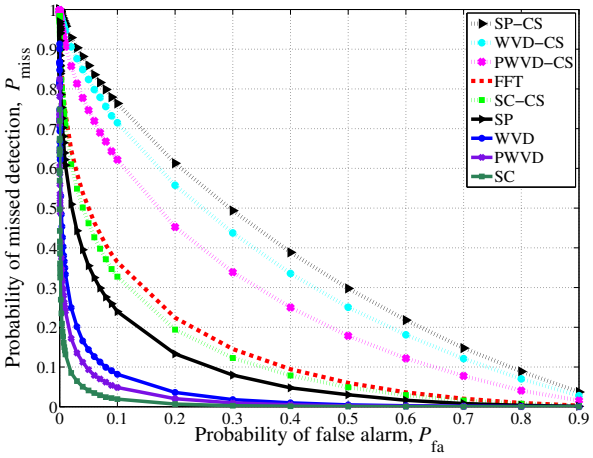

Fig. 7: The complementary ROC curves of proposed TF compressed detectors compared to TF detectors and FFT detector for SNR $= -5\,\text{dB}$ in AWGN channel.

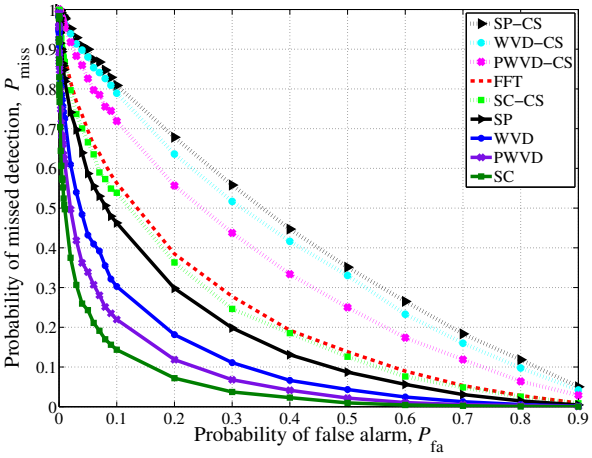

Fig. 9: The complementary ROC curves of proposed TF compressed detectors compared to TF detectors and FFT detector for SNR $= -5\,\text{dB}$ in Rician Fading.

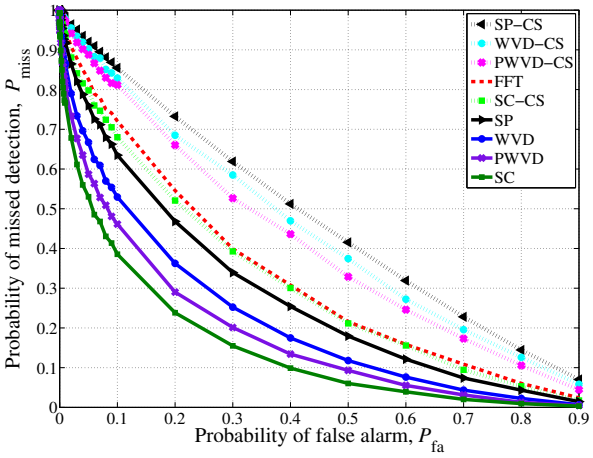

Fig. 8: The complementary ROC curves of proposed TF compressed detectors compared to TF detectors and FFT detector for SNR $= -5\,\text{dB}$ in Rayleigh Fading.

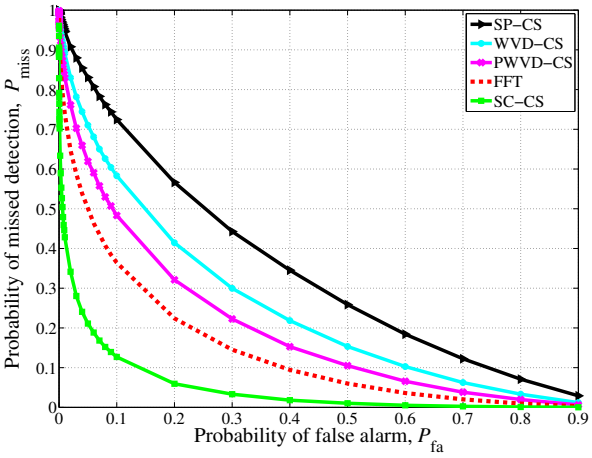

Fig. 10: The complementary ROC curves of proposed TF compressed detectors with BCS reconstruction algorithm compared to FFT detector for SNR $= -5\,\text{dB}$ in AWGN channel.

be detected at such an SNR using the WVD, whereas we can still distinguish the presence of the PU signal for other TFRs.

Figure 5 and 6 illustrate the recovery of the SP and WVD of DTV signal in noise free scenario, respectively, by minimizing the ℓ_1-norm for different $\text{card}(\Omega)/N^2$. These simulations justify that too small cardinality does not gain enough information about the DTV signal, on the other hand, too large one makes more computational complexity. The best choice of $\text{card}(\Omega)/N^2$ for the recovery of the SP of DTV signal is 0.01 to achieve reasonably efficient solution in the minimum ℓ_1-norm method. Since the cross-terms have negative effects on signal recovery, the perfect cardinality for the recovery of the WVD of DTV signal can be chosen as $\text{card}(\Omega)/N^2 = 0.25$, which is greater than cardinality for the recovery of the SP of DTV signal.

Figure 7 depicts the complementary ROC of different detectors for SNR $= -5\,\text{dB}$ in AWGN channel based on Montecarlo method by 10^4 independent runs. The proposed TF compressed detectors have been compared to TF detectors and FFT detector. As can be seen, the TF detectors perform better than single domain detector (FFT detector). Also, the detection based on the SC outperforms the detection based on the SP, WVD and PWVD. The TF compressed detectors are plotted for the relative sparsity measure $\text{card}(\Omega)/N^2 = 0.1$, hence we can achieve fast detection. However, the evaluation shows that the performance of TF compressed detectors are worse than TF detectors, because the minimum ℓ_1-norm is sensitive to noise. As can be seen, the detection performance based on the SC is significantly better than other TF compressed detectors.

Besides, this detector outperforms the FFT detector. Note that, CS makes greater reduction in the performance of the WVD detector than the other TF detectors caused by the cross terms.

Since the AWGN channel may not be valid in practical wireless channels, we examine the performance of proposed TF compressed detectors under Rayleigh and Rician fading models. We assume a single path flat fading channel with maximum Doppler shift of $100\,\mathrm{Hz}$ and Rician K-factor value 4. For generating Rayleigh and Rician channels, we use the Matlab's *rayleighchan* and *ricianchan* functions. The ROCs for TF compressed spectrum sensing techniques under Rayleigh and Rician fading models are given in Figure 8 and Figure 9, respectively. As can be observed, AWGN channel has better performance than Rayleigh and Rician fading channels and Rayleigh fading channel has lower performance than AWGN and Rician fading channels.

Figure 10 demonstrates the performance of TF compressed detectors with BCS reconstruction algorithm for SNR $= -5\,\mathrm{dB}$ in AWGN channel. By comparison, we can conclude that TF compressed detectors with the BCS outperform the BP.

V. Conclusion

The paper proposed a novel approach for spectrum sensing that suggests the use of TF analysis, which gives improvement in temporal and spectral resolution simultaneously, however on the other hand, the computational cost will be increased significantly. Therefore, we exploit CS to reduce the extremely high sampling rate of signal in TF plane. CS makes the reduction in the performance of TF detectors, but the new TF detectors have lower computational complexity than TF detectors. The simulation results demonstrated the performance of the proposed TF compressed detectors compared to existing detectors utilizing the BP and BCS reconstruction algorithms for AWGN and also Rayleigh and Rician fading channels and it was observed that the TF compressed detectors with the BCS reconstruction algorithm outperform the BP based ones.

VI. Acknowledgement

The work of Tamer Khattab is supported by Qatar National Research Fund (QNRF) under the National Priorities Research Program (NPRP) grant number NPRP 09-1168-2-455.

References

[1] L. Cohen, "Time frequency distribution: A review," *in Proceedings of IEEE*, vol. 77, no. 7, pp. 941–981, July 1989.

[2] F. Auger, P. Flandrin, P. Goncalves, and O. Lemoine, *Time-Frequency Toolbox Tutorial*. CNRS (France), Rice University (USA), 2005.

[3] Y. Luo and Z. Bu, "Distributed spectrum sensing based on the gabor time-frequency analysis for cognitive networks," *IET International Communication Conference on Wireless Mobile and Computing (CCWMC)*, pp. 690–693, 2009.

[4] W. Guibene and A. Hayar, "Joint time-frequency spectrum sensing for cognitive radio," *International Symposium on Applied Sciences in Biomedical and Communication Technologies*, pp. 1–4, 2010.

[5] F. Javed and A. Mahmood, "The use of time frequency analysis for spectrum sensing in cognitive radios," *Signal Processing and Communication Systems (ICSPCS)*, pp. 1–7, 2010.

[6] A. Chandran, A. Karthik, A. Kumar, M. S. Siva, U. S. Iyer, R. Ramanathan, and R. C. Naidu, "Discrete wavelet transform based spectrum sensing in futuristic cognitive radios," *International Conference Devices and Communications (ICDeCom)*, pp. 1–4, 2011.

[7] E. J. Candes and M. B. Wakin, "An introduction to compressive sampling," *IEEE Signal Processing Magazine*, vol. 25, no. 2, pp. 21–30, 2008.

[8] V. Havary-Nassab, S. Hassan, and S. Valaee, "Compressive detection for wide-band spectrum sensing," in *Proceedings of IEEE International Conference on Acoustics, Speech and Signal Processing (ICASSP)*, 2010, pp. 3094–3097.

[9] S. S. M. Monfared, A. Taherpour, and T. Khattab, "Compressed wide-band spectrum sensing with correlated subband occupancy in multi-antenna cognitive radios," *23nd International Symposium on Personal, Indoor and Mobile Radio Communications (PIMRC2012)*, pp. 2195–2201, 2012.

[10] P. Borgnat and P. Flandrin, "Time-frequency localization from sparsity constraints," in *Proceedings of the IEEE International Conference on Acoustics, Speech, and Signal Processing (ICASSP)*, 2008, pp. 3785–3788.

[11] P. Flandrin and P. Borgnat, "Time-frequency energy distributions meet compressed sensing," *IEEE Transactions on Signal Processing*, vol. 58, no. 6, pp. 2974–2982, 2010.

[12] S. Stankovic, I. Orovic, and M. Amin, "Compressed sensing based robust time-frequency representation for signals in heavy-tailed noise," *11th International Conference on Information Science, Signal Processing and their Applications (ISSPA)*, pp. 605–610, 2012.

[13] I. Orovic, S. Stankovic, and M. Amin, "Compressive sensing for sparse time-frequency representation of nonstationary signals in the presence of impulsive noise," *SPIE Defense, Security and Sensing*, Baltimore, Maryland, United States, 2013.

[14] X. Xiao-Chun, "Compressive sensing based measurement of time-frequency shifts system," in *Proceedings of the IEEE International Conference on Wireless Communications, Networking and Information Security (WCNIS)*, 2010, pp. 94–97.

[15] G. E. Pfander and H. Rauhut, "Sparsity in time-frequency representations," *Computing Research Repository (CORR)*, vol. abs/0711.2503, 2007.

[16] S. S. Chen, D. L. Donoho, and M. A. Saunders, "Atomic decomposition by basis pursuit," *Society for Industrial and Applied Mathematics Journal on Scientific Computing*, vol. 43, no. 1, pp. 129–159, 2001.

[17] S. Ji, Y. Xue, and L. Carin, "Bayesian compressive sensing," *IEEE Transactions on Signal Processing*, vol. 56, no. 6, 2008.

[18] C. La and M. N. Do, "Signal reconstruction using sparse tree representations," *Symposium on Optical Science and Technology, Wavelets XI*, vol. 5914, pp. 1–11, Sept. 2005.

[19] M. B. Shamsollahi, L. Senhadji, and R. L. Bouquin-Jeannes, "Time-frequency analysis: a comparison of approaches for complex EEG patterns in epileptic seizures," *IEEE 17th Annual Conference on Engineering in Medicine and Biology Society*, 1995.

[20] P. Gonçalves and R. Baraniuk, "Pseudo affine wigner distributions: Definition and kernel formulation," *IEEE Trans. on Signal Processing*, vol. 46, no. 6, pp. 2305–2314, June 1998.

[21] E. J. Cands, J. K. Romberg, and T. Tao, "Robust uncertainty principles: exact signal reconstruction from highly incomplete frequency information," *IEEE Transactions on Information Theory*, vol. 52, no. 2, pp. 489–509, 2006.

[22] http://tftb.nongnu.org.

[23] E. Candes and J. Romberg, "ℓ_1-magic: Recovery of sparse signals via convex programming," Users Guide of the ℓ_1-MAGIC toolbox for MATLAB, http://www.acm.caltech.edu/l1magic/, 2005.